Making connections with molecular wires: extending tri-nickel chains with axial cyanide, dicyanamide, and phenylacetylide ligands†

John F. Berry, F. Albert Cotton* and Carlos A. Murillo*

Laboratory for Molecular Structure and Bonding, Department of Chemistry, Texas A&M University, College Station, TX 77843-3255, USA

New chemistry needed to facilitate the replacement of axial ligands (X) in $Ni_3(dpa)_4X_2$ complexes (dpa = the anion of dipyridylamine) has been explored and used to replace X = Cl by X = CN, NCNCN, and C≡CPh. The resulting compounds, **3**, **4**, and **5**, respectively, have been characterized by X-ray crystallography and cyclic voltammetry, *inter alia*. It is found that both the mean Ni · · · Ni separations (*D*), and the magnitude of the antiferromagnetic coupling (*J*) between the terminal, high spin (*S* = 1) Ni(II) atoms vary in a correlated way, with |*J*| decreasing with increasing *D*. The relationship is nearly linear over the available ranges of parameters, suggesting that the coupling may proceed mainly through the central, diamagnetic Ni(II) ion.

Introduction

In recent years, linear trinuclear complexes of the type $M_3(dpa)_4Cl_2$(dpa = 2,2′-dipyridylamine, see Scheme 1) have been studied in this[1–4] and other[5–7] laboratories as the prototypical examples of *extended metal atom chains*[8–10] (EMACs) based on polypyridylamido ligands.[11] The impetus for this research is to develop a fundamental understanding of the metal–metal bonding in simple chains so that it will become clear, by analogy, what properties to expect from chains of much greater length. Because of the potential conducting properties of these chains, EMACs may be useful as molecular wires or devices in a "bottom-up" approach to nanoscale electronics.[12]

dipyridylamide
(dpa)

M = Cr, Co, Ni, Cu, Ru, Rh
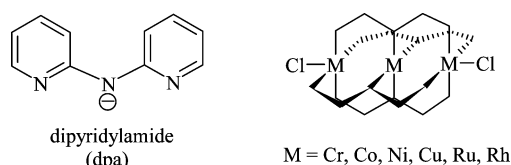
Scheme 1

While studying the $M_3(dpa)_4X_2$ compounds, we have also studied the one-electron oxidized species $[Cr_3(dpa)_4Cl_2]^+$,[13] $[Co_3(dpa)_4Cl_2]^+$,[14] $[Ni_3(dpa)_4]^{3+}$,[15] and $[Cu_3(dpa)_4Cl_2]^+$.[16] The $[Ni_3(dpa)_4]^{2+/3+}$ couple is particularly interesting because there are no Ni–Ni bonds in $Ni_3(dpa)_4Cl_2$ (**1**; Ni · · · Ni ≈ 2.43 Å), but upon oxidation, the product, $[Ni_3(dpa)_4][PF_6]_3$, has Ni–Ni distances 0.15 Å shorter (2.28 Å) than in the Ni_3^{6+} species, clearly indicative of delocalized Ni_3 bond formation. This opens the possibility of using compounds or materials incorporating this couple as insulator/conductor switches for application in molecule-scale diodes, rheostats, *etc*. For polynickel complexes to serve as molecular "wires," however, it must be possible to connect things together with them. This implies complete control of substitution reactions in the axial positions. To ascertain whether $M_3(dpa)_4X_2$ compounds are actually conducting at the molecular level, it should be possible to attach a donor molecule to one end of the chain and an acceptor molecule to the other to see if these can "talk" to each other.

Towards this end, a general synthetic strategy is presented here for exchanging the axial ligands of $[Ni_3(dpa)_4]^{2+}$ compounds using $[Ni_3(dpa)_4(NCMe)_2][PF_6]_2$ (**2**), a compound with labile acetonitrile ligands in the axial positions. This has been used to synthesize $Ni_3(dpa)_4(CN)_2$ (**3**), $Ni_3(dpa)_4(NCNCN)_2$ (**4**), and $Ni_3(dpa)_4(C≡CPh)_2$ (**5**). Since lower oxidation potentials are desirable to yield greater stability in the oxidized species, the electrochemistry of the new compounds has been studied. Also presented are the magnetic properties of the new compounds, along with comparisons to the known Ni_3^{6+} compounds, and a mechanism for the antiferromagnetic coupling in these compounds is suggested.

Experimental

General

All manipulations were carried out under an atmosphere of dry nitrogen gas using standard Schlenk techniques. Solvents were distilled in a nitrogen atmosphere over appropriate drying agents prior to use. $Ni_3(dpa)_4Cl_2$[16] and $[Ni_3(dpa)_4(NCMe)_2]$-$[PF_6]_2$[17] were prepared according to previously reported methods. Sodium cyanide, sodium dicyanamide, and phenylacetylene were purchased from Aldrich and used as received. Phenylacetylene was stored in a refrigerator over molecular sieves.

Physical measurements

IR spectra were collected on a Perkin-Elmer 16PC FTIR spectrometer using KBr pellets. Cyclic voltammograms were measured using a CH Instruments electrochemical analyser from 1 M NBu_4PF_6 solutions in CH_2Cl_2 which were 0.05 mM in **3**–**5**. Compound **5** was also studied in THF solution. The electrodes were: Pt disk (working), Pt wire (auxiliary), and Ag/AgCl (reference). Elemental analyses for **3**–**5** were carried out by Canadian Microanalytical Services, British Columbia, Canada. These were all satisfactory.

Magnetic susceptibility measurements for **3**–**5** were made on crushed crystalline samples from which the interstitial solvents had been removed under vacuum. The samples were carefully weighed and placed in a plastic bag, which was mounted in a drinking straw and then placed inside a Quantum Design MPMS-XL SQUID magnetometer. Variable temperature data were collected from 2 to 300 K at a field of 1000 G for **4** and **5**, and at 10 000 G for **3**. The data were corrected empirically for the diamagnetism of the sample and the holder.

† Electronic supplementary information (ESI) available: experimental preparations and crystal data for the partially substituted complexes $Ni_3(dpa)_4Cl(BF_4)$, $Ni_3(dpa)_4(CN)_xCl_{2-x}$, $Ni_3(dpa)_4(CCPh)_x$-$(OH)_yCl_{2-x-y}$, and $Ni_3(dpa)_4(CCPh)_xCl_{2-x}$. See http://www.rsc.org/suppdata/dt/b3/b305258c/

Syntheses

Preparation of Ni$_3$(dpa)$_4$(CN)$_2$ (3). To a mixture of [Ni$_3$-(dpa)$_4$(NCMe)$_2$][PF$_6$]$_2$ (**2**) (0.050 g, 0.041 mmol) and NaCN (0.005 g, 0.1 mmol) was added 15 mL of methanol. After stirring the resulting purple solution for 3 h at room temperature, the solvent was removed under vacuum and the residue was extracted with 5 mL of dichloromethane. After filtration, the clear purple filtrate was layered with hexanes. Dark block-shaped crystals, about a millimeter in width, of **3**·CH$_2$Cl$_2$ grew in about a week. Yield: 22 mg, 59%. IR (KBr, cm^{-1}): 3448 (m, br), 3025 (w), 2120 (w, C≡N), 1602 (s), 1547 (m), 1467 (vs), 1424 (vs), 1363 (s), 1312 (m), 1282 (m), 1244 (w), 1154 (m), 1053 (w), 1013 (m), 892 (w), 765 (m), 738 (m), 639 (w), 518 (w), 428 (w). Anal. calcd. for Ni$_3$C$_{43}$H$_{34}$N$_{14}$Cl$_2$: C, 51.97; H, 3.42; N, 19.74; found: C, 52.01; H, 3.32; N, 19.60%. ESI(+)-MS (*m/z*): 882 [M − CN]$^+$.

Preparation of Ni$_3$(dpa)$_4$(NCNCN)$_2$ (4). To a mixture of **2** (0.038 g, 0.031 mmol) and NaNCNCN (0.007 g, 0.08 mmol) was added 10 mL of methanol. After stirring the resulting purple solution for 3 h at room temperature, the solvent was removed under vacuum and the residue was extracted with 5 mL of dichloromethane. After filtration, the clear purple filtrate was layered with hexanes (30 mL). Purple plate-like crystals of **4**·2.5CH$_2$Cl$_2$ grew within a week. Yield: 20 mg, 65%. IR (KBr, cm^{-1}): 3448 (m, br), 2964 (w), 2276 (m, C≡N), 2220 (m, C≡N), 2165 (vs, C≡N), 1602 (s), 1547 (m), 1465 (vs), 1424 (vs), 1357 (s), 1311 (m), 1263 (m), 1154 (m), 1049 (m, br), 1016 (m), 893 (w), 803 (m), 763 (m), 741 (m), 640 (w), 515 (w), 428 (w). Anal. calcd. for Ni$_3$C$_{45.25}$H$_{345}$N$_{18}$Cl$_{25}$: C, 49.63; H, 3.18; found: C, 49.60; H, 3.23%. ESI(+)-MS (*m/z*): 922 [M − NCNCN]$^+$.

Preparation of Ni$_3$(dpa)$_4$(C≡CPh)$_2$, (5). Methanol (20 mL) was added to **2** (0.200 g, 0.163 mmol), resulting in a dark purple suspension. To this was added 408 μL (408 mmol) of a 1 M NaOH solution in methanol. After swirling the mixture, a clear wine-red solution resulted. A solution of phenylacetylene (200 μL, 2.10 mmol) in 5 mL of methanol was then added and the resulting red solution was allowed to stand without stirring. Dark red crystals of **5**·0.3MeOH grew from this solution over the course of four days. The crystals were collected, washed with ethanol (10 mL) and hexanes (10 mL), and dried under vacuum. Yield: 143 mg, 83%. IR (KBr, cm^{-1}): 3448 (m, br), 3060 (w), 3020 (w), 2081 (w, C≡C), 1601 (s), 1590 (s), 1548 (m), 1466 (vs), 1422 (vs), 1364 (s), 1310 (m), 1280 (m), 1243 (w), 1201 (w), 1152 (s), 1051 (w), 1011 (m), 891 (w), 844 (w), 762 (s), 740 (m), 693 (w), 637 (w), 518 (w), 428 (m). Anal. calcd. for Ni$_3$C$_{56.5}$H$_{43}$N$_{12}$Cl: C, 61.60; H, 3.91; N, 15.26; found: C, 61.34; H, 3.93; N, 15.77%. ESI(+)-MS (*m/z*): 957 [M − C≡CPh]$^+$.

X-Ray crystallographic determinations

In each case, a suitable crystal was mounted on the end of a quartz fiber using a small amount of grease and transferred to the goniometer of a Bruker SMART 1000 CCD area detector system, where it was cooled to −60 °C for the duration of the experiment. Initial unit cell parameters were obtained from SMART[18] software. Data integration, correction for Lorentz and polarization effects, and final cell refinement were performed with SAINTPLUS.[19] The data were further corrected for absorption using SADABS.[20]

For **3**·CH$_2$Cl$_2$ and **5**·0.3CH$_3$OH, the initial structure solutions were obtained by the direct methods routine in SHELXTL.[21] For **4**·2.5CH$_2$Cl$_2$, the Patterson method was used. Subsequent refinement cycles (based on F^2) and Fourier synthesis revealed the positions of all the non-hydrogen atoms. These atoms (with the exception of disordered groups) were refined using anisotropic displacement tensors. All hydrogen atoms were added in calculated positions for the final refinement cycle. The stereochemical configuration of **3**·CH$_2$Cl$_2$ was

determined by selecting the configuration which gave a Flack parameter of zero,[22] whereas **5**·0.3CH$_3$OH was refined as a racemic twin.

Thermal ellipsoid plots of **3**·CH$_2$Cl$_2$, **4**·2.5CH$_2$Cl$_2$, and **5**·0.3CH$_3$OH are shown in Fig. 1, 2, and 3, respectively. Table 1 lists the pertinent crystallographic data and Table 2 gives the important interatomic distances.
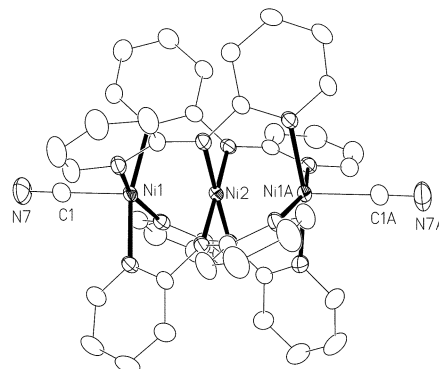

Fig. 1 Thermal ellipsoid plot of **3** with ellipsoids drawn at 50% probability. Hydrogen atoms are omitted for clarity.
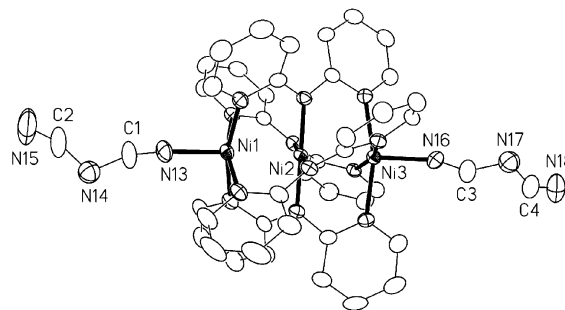

Fig. 2 Thermal ellipsoid plot of **4** with ellipsoids drawn at 50% probability. Hydrogen atoms are omitted and only one orientation of the disordered groups is shown.
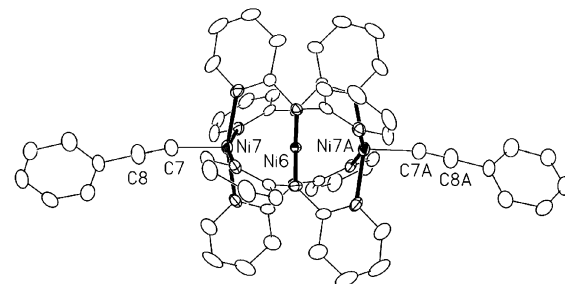

Fig. 3 Thermal ellipsoid plot of one of the three independent molecules of **5** in **5**·0.3MeOH. Hydrogen atoms are omitted for clarity and ellipsoids are drawn at 50% probability.

CCDC reference numbers 207897–207899.

See http://www.rsc.org/suppdata/dt/b3/b305258c/ for crystallographic data in CIF or other electronic format.

Results and discussion

Synthesis of Ni$_3$(dpa)$_4$(X)$_2$ (X = CN$^-$, NCNCN$^-$)

In our study of Co$_3$(dpa)$_4$X$_2$ compounds,[23] Co$_3$(dpa)$_4$(BF$_4$)$_2$ was found to be the crucial starting material which allowed facile substitution of the axial BF$_4$ anions by other ligands (*e.g.* CN$^-$, NCS$^-$, NCNCN$^-$),[23] as shown in eqn. 1 and 2.
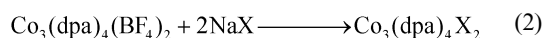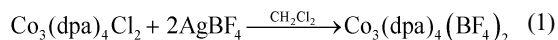
$$Co_3(dpa)_4Cl_2 + 2AgBF_4 \xrightarrow{CH_2Cl_2} Co_3(dpa)_4(BF_4)_2 \quad (1)$$

$$Co_3(dpa)_4(BF_4)_2 + 2NaX \longrightarrow Co_3(dpa)_4X_2 \quad (2)$$

Table 1 Crystal data for **3–5**

|	Ni$_3$(dpa)$_4$(CN)$_2$·CH$_2$Cl$_2$ 3·CH$_2$Cl$_2$	Ni$_3$(dpa)$_4$(NCNCN)$_2$·2.5CH$_2$Cl$_2$ 4·2.5CH$_2$Cl$_2$	Ni$_3$(dpa)$_4$(CCPh)$_2$·0.3CH$_3$OH 5·0.3CH$_3$OH
Formula	C$_{43}$H$_{34}$Cl$_2$N$_{14}$Ni$_3$	C$_{46.5}$H$_{37}$Cl$_5$N$_{18}$Ni$_3$	C$_{56.3}$H$_{43.2}$N$_{12}$Ni$_3$O$_{0.3}$
FW	993.87	1201.32	1068.76
Crystal system	Orthorhombic	Triclinic	Monoclinic
Space group	$Pnn2$	$P\bar{1}$	$C2$
a/Å	13.016(1)	11.3181(8)	37.149(3)
b/Å	14.069(1)	11.9122(9)	15.866(1)
c/Å	11.494(1)	20.792(2)	17.149(1)
a/°	90	102.830(1)	90
β/°	90	91.261(2)	92.435(2)
γ/°	90	111.566(1)	90
V/Å^3	2104.9(3)	2525.2(3)	10098(1)
Z	2	2	8
d(calc)/g cm^{-3}	1.568	1.58	1.406
$R1,^a wR2^b$ ($I > 2\sigma I$)	0.0228, 0.0588	0.0583, 0.1207	0.0465, 0.1047
$R1,^a wR2^b$ (all data)	0.0238, 0.0598	0.0943, 0.1397	0.0700, 0.1164

^{a} $R1 = ||\Sigma F_o| - |F_c|| / \Sigma |F_o|$. ^{b} $wR2 = [\Sigma[w(F_o^2 - F_o^2)^2]/\Sigma[w(F_o^2)^2]]^{1/2}$; $w = 1/\sigma^2(F_o^2) + (aP)^2 + bP$, where $P = [\max(0 \text{ or } F_o^2) + 2(F_c^2)]/3$.

Table 2 Selected bond distances (Å) for **3–5**

	3·CH$_2$Cl$_2$	4·2.5CH$_2$Cl$_2$	5·0.3CH$_3$OH
Ni · · · Ni	2.4523(3)	2.4044(8)	2.477(1)
		2.4082(8)	2.474(1)
			2.4861(7)
			2.4467(8)
Ni–N$_{outer}$	2.091(2)	2.089[4]	2.104[6]
Ni–N$_{inner}$	1.902(2)	1.883[3]	1.894[6]
Ni–X$_{ax}$	2.014(2)	2.029[4]	2.00[1]
C≡N or C≡C	1.146(3)	1.124[7]	1.19[2]

It would be expected that Ni$_3$(dpa)$_4$X$_2$ compounds could be made similarly. However, isolation of Ni$_3$(dpa)$_4$(BF$_4$)$_2$ has not been possible. Reaction of Ni$_3$(dpa)$_4$Cl$_2$ with two equivalents of AgBF$_4$ resulted in complete substitution of only one of the axial chloride ions (see ESI†). Reaction with excess TlBF$_4$[24] gives the same result. Thus, a new strategy was necessary for the synthesis of Ni$_3$(dpa)$_4$X$_2$ compounds.

Recently, we reported that Co$_3$(depa)$_4$Cl$_2$ [depa = di-2,2′-(4-ethyldipyridyl)amide] can be converted directly to Co$_3$(depa)$_4$-(CN)$_2$ without the use of a tetrafluoroborate intermediate simply by stirring together Co$_3$(depa)$_4$Cl$_2$ and a forty-fold excess of NaCN in a mixture of methanol and acetone at room temperature.[25] Under similar conditions, Ni$_3$(dpa)$_4$Cl$_2$ also reacts with NaCN, and single crystals of the product of this reaction were analyzed. From the initial solution of the crystal structure, this product appeared to be Ni$_3$(dpa)$_4$(CN)$_2$, but the displacement parameters for the axial ligands were physically unreasonable: those for the carbon atoms were too small and those for the nitrogen atoms were too big. The reason for this is that there is only partial substitution of the axial Cl$^-$ ions (see Fig. 4). Thus, the complex is best formulated as Ni$_3$(dpa)$_4$-(CN)$_x$Cl$_{2-x}$ (see ESI†). Yet another synthetic strategy was necessary to eliminate this problem.
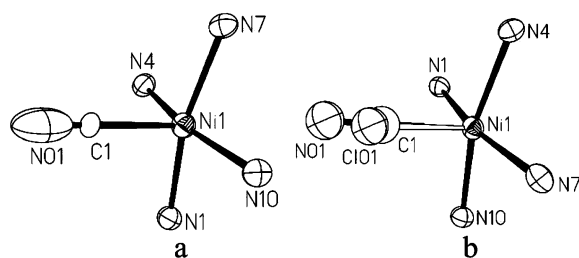
Fig. 4 Thermal ellipsoid plots of a terminal NiN$_4$CN unit from Ni$_3$(dpa)$_4$(CN)$_x$Cl$_{2-x}$ before (a) and after (b) resolving the disorder in the axial ligands.

The compound Ni$_3$(dpa)$_4$Cl$_2$ has been shown to react cleanly with AgPF$_6$ in acetonitrile to give [Ni$_3$(dpa)$_4$(NCMe)$_2$][PF$_6$]$_2$ (**2**), an ionic species which is slightly soluble in methanol.[17] Using this acetonitrile complex, it is possible to prepare Ni$_3$-(dpa)$_4$X$_2$ compounds without chloride impurities (eqn. 3).

$$[Ni_3(dpa)_4(NCMe)_2][PF_6]_2 + 2NaX \xrightarrow{\text{MeOH}}$$
$$Ni_3(dpa)_4X_2 + 2NaPF_6 + 2MeCN \quad (3)$$
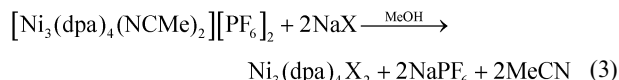
In the examples reported here, X is cyanide or dicyanamide (compounds **3** and **4**, respectively). This reaction, however, should be quite general and applicable to a large range of X anions. The only limitation is that X must be narrow enough to fit in the axial position without causing steric crowding.

Synthesis of Ni$_3$(dpa)$_4$(C≡CPh)$_2$

Transition metal acetylide complexes have recently been of interest,[26] especially in organometallic chemistry,[27] as have metal–metal bonded dinuclear compounds containing acetylide ligands.[28] Synthesis of [M$_3$(dpa)$_4$]$^{2+}$ complexes with axial acetylide anions represents extension of this chemistry to EMAC compounds. The first bis-acetylide complex of an [M$_3$(dpa)$_4$]$^{2+}$ core was synthesized[29] in this laboratory according to eqn. 4.

$$Cr_3(dpa)_4Cl_2 + 2LiCCPh \xrightarrow{\text{THF}}$$
$$Cr_3(dpa)_4(CCPh)_2 + 2LiCl \quad (4)$$
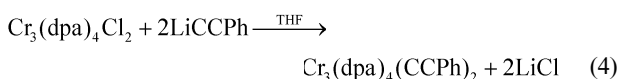
Analogous reactions with Ni$_3$(dpa)$_4$Cl$_2$ led only to intractable products. After numerous unsuccessful reactions between **1**, phenylacetylene, and various bases, the following reaction (eqn. 5) afforded single crystals of what appeared to be Ni$_3$(dpa)$_4$-(C≡CPh)$_2$ from dichloromethane solution, albeit in only 5% yield.

$$Ni_3(dpa)_4Cl_2 + 2NaOH + 2HCCPh \xrightarrow{\text{MeOH}}$$
$$Ni_3(dpa)_4(CCPh)_x(OH)_yCl_{2-x-y} \quad (5)$$
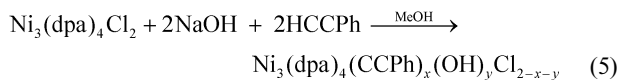
However, careful inspection of the crystal structure revealed that the axial positions of the molecule were disordered with partially occupied chloride, hydroxide, and phenylacetylide groups, as shown in Fig. 5 (see also ESI†). In an attempt to remove chloride from the reaction, we used TlPF$_6$ and found that the product of the reaction crystallized from methanol solution (eqn. 6).
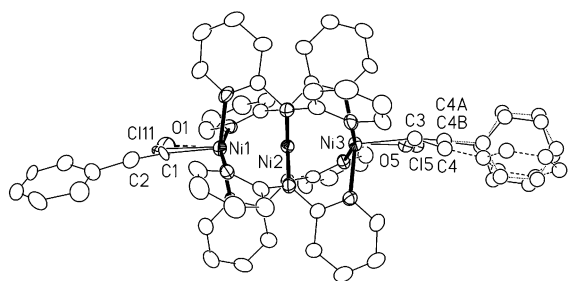
$$Ni_3(dpa)_4Cl_2 + 2NaOH + 2HCCPh + 2TlPF_6 \xrightarrow{\text{MeOH}}$$
$$Ni_3(dpa)_4(CCPh)_xCl_{2-x} \quad (6)$$

Fig. 5 Thermal ellipsoid plot of $Ni_3(dpa)_4Cl_x(OH)_y(C\equiv CPh)_{2-x-y}$ with all disordered groups shown. Hydrogen atoms are omitted for clarity.

Unfortunately, chloride ions were *still* found in the crystal partially occupying the axial position of the Ni_3 unit (see ESI†). However, the percentage of phenylacetylide ligands was 85%, greater than the 68% found in crystals obtained using the conditions in eqn. 5. Importantly, no hydroxide was detected in the axial positions, as confirmed by the absence of O–H stretching vibrations in the IR spectrum of the solid.

Thus, for a clean reaction, it was clear that a starting material containing no chloride was required. Compound **2** fulfils this requirement and gave a pure product in high (>80%) yields (eqn. 7).

$$Ni_3(dpa)_4(NCMe)_2(PF_6)_2 + 2NaOH + 2HCCPh \xrightarrow{\text{MeOH}}$$

$$Ni_3(dpa)_4(CCPh)_2 \quad (7)$$
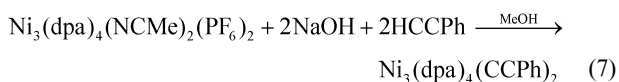
Although no intermediates in the reaction were isolated, we postulate the bis-hydroxo complex as the key intermediate in the reaction, as shown in Scheme 2. The reasons for this presumption are: (i) while **2** is not very soluble in methanol, addition of NaOH gives a clear solution, indicating the formation of a new soluble complex; (ii) under the conditions of eqn. 5, hydroxide ligands have been detected by crystallography in the product (see eqn. 5).
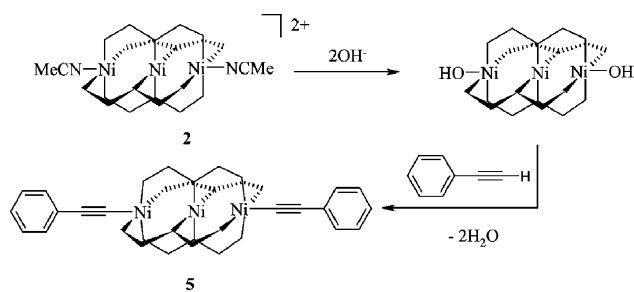
Scheme 2

Structural results

Crystals of $3 \cdot CH_2Cl_2$ form in the non-centrosymmetric space group $Pnn2$, isomorphous to the previously reported Co_3 analog. The compound has crystallographically imposed twofold symmetry, the axis passing through the central nickel atom perpendicular to the Ni_3 chain. This gives a unique Ni $\cdots$ Ni distance of 2.4523(3) Å, which is ~0.1 Å longer than the Co–Co distance in the isomorphous $Co_3(dpa)_4(CN)_2$ [2.3392(2) Å].[23]

Compound **4** crystallizes on a general position in the space group $P\bar{1}$. Thus, the crystal contains a racemic mixture of the Λ and Δ enantiomers, the two being related by a center of symmetry. Here, there are two independent Ni $\cdots$ Ni distances, which are statistically equivalent [2.4044(8) and 2.4082(8) Å], with a mean value of 2.406[1] Å. These are also ~0.1 Å longer than those in the analogous tricobalt complex.[23]

Table 3 Oxidation potentials for $Ni_3(dpa)_4X_2$ compounds in CH_2Cl_2 solution

Compound	$E_{\frac{1}{2}}$/V (*vs.* Ag/AgCl)
$Ni_3(dpa)_4Cl_2$ (**1**)	0.908 [a]
$[Ni_3(dpa)_4(NCMe)_2][PF_6]_2$ (**2**)	1.205 [b]
3	0.975
4	1.147
5	0.767
	0.860 [c]

[a] Data from ref. 15. [b] Data from ref. 17. [c] THF solution.

Compound **5** crystallizes in the non-centrosymmetric space group $C2$ with $Z = 8$. Thus, the asymmetric unit contains two molecules of **5**. One is a whole molecule of **5** and the other is formed by two unconnected halves of the molecule with the central Ni atoms lying along the independent twofold axes at $(\frac{1}{2}, y, \frac{1}{2})$ and $(0, y, \frac{1}{2})$ for Ni(5) and Ni(6), respectively. The average of the four independent Ni $\cdots$ Ni distances, 2.4709[9] Å, is longer than the Cr–Cr distances in $Cr_3(dpa)_4(C\equiv CPh)_2$[29] (2.419[2] Å) by ~0.05 Å, as expected, since the trinickel analog has no Ni–Ni bonds.

Compounds **3–5** have the typical helicoidal geometry of the $Ni_3(dpa)_4^{n+}$ compounds.[3,16,17] The outer Ni–N distances are typically >0.1 Å longer than the inner Ni–N distances, since the former Ni atoms are five coordinate and high spin,[3,16] and the Ni $\cdots$ Ni separations in the compounds appear to vary according to the donor strength of the axial ligands. Since there are no Ni–Ni bonds in the Ni_3^{6+} compounds,[3] a very basic axial ligand, such as phenyl acetylide, can easily pull the terminal Ni atoms away from the central one. Conversely, a neutral donor, such as acetonitrile, leads to shorter Ni $\cdots$ Ni distances (~2.37 Å).[17] In contrast to the behaviour of $Cr_3(dpa)_4X_2$ compounds[29] and $Co_3(dpa)_4X_2$ compounds,[30] all of these $Ni_3(dpa)_4X_2$ compounds have nearly equal Ni $\cdots$ Ni distances. This again is due to the fact that there are no Ni–Ni bonds present and the axial ligands are the same.

Electrochemistry

In our previous report of the one-electron oxidation of $Ni_3(dpa)_4Cl_2$,[15] we noted that the oxidation potential for this process was quite high (0.908 V *vs.* Ag/AgCl). Also, the oxidized species is rather unstable: solutions of $[Ni_3(dpa)_4][PF_6]_3$ revert to Ni_3^{6+} within 24 h at room temperature, and the solid decomposes at room temperature in a matter of days. Thus, it would be desirable to improve the oxidizability of the Ni_3^{6+} species and the stability of the Ni_3^{7+} species. We have recently reported[17] one way to do this: addition of stabilizing ethyl groups to the dpa ligand to give depa (di-4-ethylpyridylamide) lowers the oxidation potential of $Ni_3(depa)_4Cl_2$ (**6**) by ~0.1 V as compared to that of **1**. Moreover, cold solutions of $[Ni_3(depa)_4][PF_6]_3$ are stable for about two weeks.

Since the axial ligands significantly affect the HOMO of the Ni_3^{7+} compounds,[16] it should be possible to alter the stability of the oxidized species by using different axial substituents on the trinickel chains. Also, it is important to have the same axial ligands in the Ni_3^{6+} and Ni_3^{7+} species if these compounds are to be used as molecular switches. Therefore, the cyclic voltammetry of the new Ni_3^{6+} compounds was studied and the results are shown in Fig. 6 and Table 3. It is clear that the cyanide-based ligands cause higher oxidation potentials, whereas phenylacetylide appears to stabilize the oxidized species. The reason for the solvent dependence ($E_{\frac{1}{2}} = 0.767$ V in CH_2Cl_2 *vs.* 0.860 V in THF) of this compound is unclear. We are, however, trying to obtain a $[Ni_3(dpa)_4(CCPh)_2]^+$ cation in crystalline form.

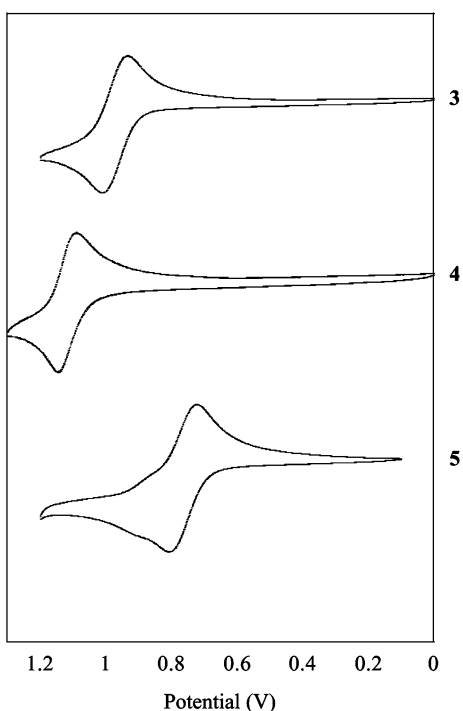**Fig. 6** Cyclic voltammograms of **3**–**5** in CH$_2$Cl$_2$ with 1 M NBu$_4$PF$_6$ electrolyte. The potentials are referenced to the Ag/AgCl electrode.

Magnetic properties

The magnetic properties of the precursors Ni$_3$(dpa)$_4$Cl$_2$ (**1**) and [Ni$_3$(dpa)$_4$(NCMe)$_2$][PF$_6$]$_2$ (**2**) have been described in detail already.[3,17] Since there are no Ni–Ni bonds in these compounds, the three Ni^{2+} ions behave independently. The central Ni atom lies in square planar coordination, and is therefore diamagnetic. The terminal Ni atoms are high spin and square pyramidal in coordination with two unpaired electrons each. The unpaired electrons at the ends of the molecule couple antiferro-magnetically.[3,17]

The magnetic susceptibility data for **3**–**5** also show this behaviour (see Fig. 7). At low temperatures, χT tends toward zero, indicating an $S = 0$ ground state. The values of χT increase as the temperature is raised, and the room temperature values are less than would be expected for two independent $S = 1$ centers (*i.e.* 2.00 emu K mol^{-1}), indicating that while the anti-ferromagnetic coupling is fairly strong, the spins are still only partially randomized at room temperature.

These data were modeled using the spin Hamiltonian, $\mathscr{H} = -JS_1 \cdot S_3$, giving the following expression for the suscepti-bility:

$$\chi = \frac{6Ng^2\beta^2(e^{J/kT} + 5e^{3J/kT})}{3kT(1 + 3e^{J/kT} + 5e^{3J/kT})} \qquad (8)$$

where g is the Landé factor, N is Avogadro's number, β is the electron Bohr magneton, k is the Boltzmann constant, J is the exchange parameter, and T is temperature. The results of the least squares fits to the data are listed in Table 4. The g values for the compounds are similar to those of previously studied Ni$_3$$^{6+}$ compounds,[17] but the J values differ according to the axial ligand of the compound (*vide infra*).

Magnetic exchange mechanism

The study of the magnetic properties of the Ni$_3$$^{6+}$ compounds **3**–**5** prompted us to consider the possible pathways for the intramolecular antiferromagnetic exchange coupling between the terminal high spin Ni^{2+} ions. In the classical case of dicop-per carboxylates, the experimental evidence shows that the exchange pathway between the unpaired electrons of the copper
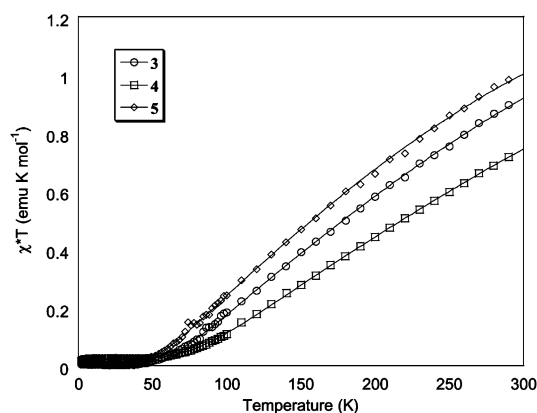

Fig. 7 Plot of χT *vs.* T for **3**–**5** in the range of 2 to 300 K. The solid lines represent least squares fits to the data using eqn. 8. The results are given in Table 4.

atoms is through the bridging carboxylate ligands, since the magnitude of the exchange parameter, J, depends not on the Cu $\cdots$ Cu distances, but on the distance through the ligand [*i.e.* Cu(1)–O(1) + O(1)–C + C–O(2) + O(2)–Cu(2)].[31] Also, the electronic properties of the bridging ligands strongly affect the magnitude of J.[32]

Comparing compounds **3**–**5**, the previously reported Ni$_3$-(dpa)$_4$Cl$_2$ (**1**) and [Ni$_3$(dpa)$_4$(NCMe)$_2$][PF$_6$]$_2$ (**2**), and also the complexes of the modified depa ligand, Ni$_3$(depa)$_4$Cl$_2$ (**6**) and [Ni$_3$(depa)$_4$(NCMe)$_2$][PF$_6$]$_2$ (**7**), the magnetic results (Table 5) suggest a different mechanism. The Ni $\cdots$ Ni distances (Table 5) in this series of compounds vary within a range of 0.1 Å, and the magnitude of J shows correlation with these distances as seen in Fig. 8. Shorter Ni $\cdots$ Ni distances lead to more negative values of J (or stronger antiferromagnetic coupling), and *vice versa*.
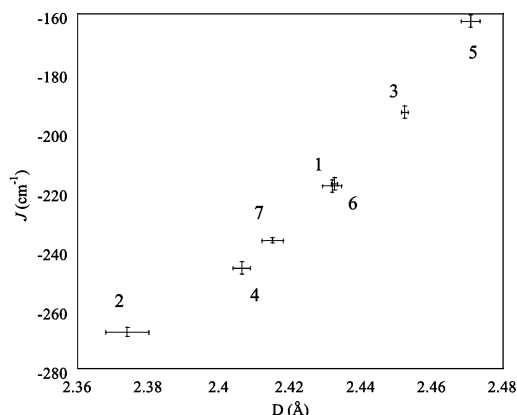

Fig. 8 Plot of the exchange parameter (J) *vs.* the Ni $\cdots$ Ni separations (D) for Ni$_3$(dpa)$_4$Cl$_2$ (**1**), [Ni$_3$(dpa)$_4$(NCMe)$_2$][PF$_6$]$_2$ (**2**), Ni$_3$(dpa)$_4$(CN)$_2$ (**3**), Ni$_3$(dpa)$_4$(NCNCN)$_2$ (**4**), Ni$_3$(dpa)$_4$(C≡CPh)$_2$ (**5**), Ni$_3$(depa)$_4$Cl$_2$ (**6**), and [Ni$_3$(depa)$_4$(NCMe)$_2$][PF$_6$]$_2$ (**7**). Error bars are drawn at 3σ. See text for interpretation.

The terminal Ni–N distances in compounds **1**–**7** fall in the narrow range 2.10 to 2.07 Å, and the other important distances for a pathway through the ligand are essentially the same. Moreover, the magnitude of the exchange parameter J does not follow the trends in the distances through this pathway. It should also be mentioned that though the ligand depa (for **6** and **7**) has been shown to be more basic than the dpa ligand,[25] this electronic effect does *not* alter the trend in J shown in Fig. 8. This is further evidence against a superexchange path-way through the ligands.

Because of the relationship between the Ni $\cdots$ Ni distances and J, it appears that the unpaired electrons on the terminal Ni atoms couple *through the central Ni atom*. This can be achieved

Table 4 Least squares fitting parameters of magnetic susceptibility data

Compound	g	J/cm^{-1}	% $S = 1$ impurity	R (goodness of fit)
3	2.084(5)	−193.2(7)	0.29(5)	0.99989
4	2.120(4)	−245.9(7)	2.32(2)	0.99995
5	2.015(6)	−162.4(7)	0.25(8)	0.99979

Table 5 Correlation of Ni · · · Ni distances with exchange parameter J

Compound	Ni · · · Ni/Å	J/cm^{-1}	Reference
$Ni_3(dpa)_4Cl_2$ (**1**)	2.4318[9]	−218.2(7)	17
$[Ni_3(dpa)_4(NCMe)_2][PF_6]_2$ (**2**)	2.374[2]	−267.6(5)	17
3	2.4523(3)	−193.2(7)	This work
4	2.4063[8]	−245.9(7)	This work
5	2.4709[9]	−162.4(7)	This work
$Ni_3(depa)_4Cl_2$ (**6**)	2.4325(3)	−217.5(7)	17
$[Ni_3(depa)_4(NCMe)_2][PF_6]_2$ (**7**)	2.415(1)	−236.6(3)	17

as follows. The d_{z^2} orbital of the central Ni atom contains an electron pair which can become spin polarized by interactions with the unpaired spins in the d_{z^2} orbitals of the terminal Ni atoms (see Scheme 3). This spin polarization leads to antiferromagnetic coupling of the electrons in the d_{z^2} orbitals. The other unpaired electron on each nickel atom (presumably in the $d_{x^2-y^2}$ orbitals) will follow suit, according to Hund's rule. This is consistent with the observed dependence of J on the Ni · · · Ni separations.
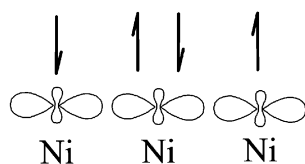
Scheme 3

Conclusions

Clean replacement of one set of axial ligands (X) in Ni_3-$(dpa)_4X_2$ by another is not generally possible in a direct way, but can be done by first converting the starting compound (in this case, X = Cl) to $[Ni_3(dpa)_4(NCMe)_2][PF_6]_2$ and then introducing the desired anionic ligand. The Ni · · · Ni separations (*D*) and the antiferromagnetic coupling parameter (*J*) both vary significantly with the identity of the axial ligands, and are inversely related, though not quite linearly. Thus, we propose that the spin–spin coupling between the terminal nickel atoms (each with $S = 1$) occurs predominantly *via* the central nickel atom.

Acknowledgements

References and notes

1 F. A. Cotton, L. M. Daniels and G. T. Jordan, IV, *Chem. Commun.*, 1997, **5**, 421.
2 F. A. Cotton, L. M. Daniels, C. A. Murillo and I. Pascual, *J. Am. Chem. Soc.*, 1997, **119**, 10223.
3 R. Clérac, F. A. Cotton, K. R. Dunbar, C. A. Murillo, I. Pascual and X. Wang, *Inorg. Chem.*, 1999, **38**, 2655.
4 J. F. Berry, F. A. Cotton, P. Lei and C. A. Murillo, *Inorg. Chem.*, 2003, **42**, 377.
5 (*a*) S. Aduldecha and B. Hathaway, *J. Chem. Soc., Dalton Trans.*, 1991, 993; (*b*) L.-P. Wu, P. Field, T. Morrissey, C. Murphy, P. Nagle, B. Hathaway, C. Simmons and P. Thornton, *J. Chem. Soc., Dalton Trans.*, 1990, 3835.
6 G. J. Pyrka, M. El-Mekki and A. A. Pinkerton, *J. Chem. Soc., Chem. Commun.*, 1991, 84.
7 (*a*) E.-C. Yang, M.-C. Cheng, M.-S. Tsai and S.-M. Peng, *J. Chem. Soc., Chem. Commun.*, 1994, 2377; (*b*) J. T. Sheu, C.-C. Lin, I. Chao, C.-C. Wang and S.-M. Peng, *Chem. Commun.*, 1996, 315.
8 (*a*) F. A. Cotton, L. M. Daniels, T. Lu, C. A. Murillo and X. Wang, *J. Chem. Soc., Dalton Trans.*, 1999, 517; (*b*) J. F. Berry, F. A. Cotton, P. Lei, T. Lu and C. A. Murillo, *Inorg. Chem.*, 2003, **42**, 3534.
9 (*a*) S.-J. Shieh, C.-C. Chou, G.-H. Lee, C.-C. Wang and S.-M. Peng, *Angew. Chem., Int. Ed. Engl.*, 1997, **36**, 56; (*b*) C.-C. Wang, W.-C. Lo, C.-C. Chou, G.-H. Lee, J.-M. Chen and S.-M. Peng, *Inorg. Chem.*, 1998, **37**, 4059; (*c*) H.-C. Chang, J.-T. Li, C.-C. Wang, T.-W. Lin, H.-C. Lee, G.-H. Lee and S.-M. Peng, *Eur. J. Inorg. Chem.*, 1999, **8**, 1243; (*d*) C.-Y. Yeh, C.-H. Chou, K.-C. Pan, C.-C. Wang, G.-H. Lee, Y.-O. Su and S.-M. Peng, *J. Chem. Soc., Dalton Trans.*, 2002, 2670.
10 These have also been referred to as "metal string complexes", see: (*a*) S.-Y. Lai, T.-W. Lin, Y.-H. Chen, C.-C. Wang, G.-H. Lee, M.-H. Yang, M.-K. Leung and S.-M. Peng, *J. Am. Chem. Soc.*, 1999, **121**, 250; (*b*) S.-Y. Lai, C.-C. Wang, Y.-H. Chen, C.-C. Lee, Y.-H. Lin and S.-M. Peng, *J. Chin. Chem. Soc. (Taipei)*, 1999, **46**, 477; (*c*) Y.-H. Chen, C.-C. Lee, C.-C. Wang, G.-H. Lee, S.-Y. Lai, F.-Y. Li, C.-Y. Mou and S.-M. Peng, *Chem. Commun.*, 1999, 1667; (*d*) S.-M. Peng, C.-C. Wang, Y.-L. Jang, Y.-H. Chen, F.-Y. Li, C.-Y. Mou and M.-K. Leung, *J. Magn. Magn. Mater.*, 2000, **209**, 80.
11 For recent reviews, see: (*a*) L.-G. Zhu and S.-M. Peng, *Wuji Huaxue Xuebao*, 2002, **18**, 117; (*b*) J. K. Bera and K. R. Dunbar, *Angew. Chem., Int. Ed.*, 2002, **41**, 4453.
12 For a recent review of molecular electronics, see: R. L. Carroll and C. B. Gorman, *Angew. Chem., Int. Ed.*, 2002, **41**, 4378.
13 R. Clérac, F. A. Cotton, L. M. Daniels, K. R. Dunbar, C. A. Murillo and I. Pascual, *Inorg. Chem.*, 2000, **39**, 752.
14 R. Clérac, F. A. Cotton, K. R. Dunbar, T. Lu, C. A. Murillo and X. Wang, *J. Am. Chem. Soc.*, 2000, **122**, 2272.
15 J. F. Berry, F. A. Cotton, L. M. Daniels and C. A. Murillo, *J. Am. Chem. Soc.*, 2002, **124**, 3212.
16 J. F. Berry, F. A. Cotton, L. M. Daniels, C. A. Murillo and X. Wang, *Inorg. Chem.*, 2003, **42**, 2418.
17 J. F. Berry, F. A. Cotton, T. Lu, C. A. Murillo and X. Wang, *Inorg. Chem.*, 2003, **42**, 3595.
18 SMART v5.05, Software for the CCD Detector System, Bruker Analytical X-Ray Systems, Inc., Madison, WI, USA, 1998.
19 SAINTPLUS v5.00, Software for the CCD Detector System, Bruker Analytical X-Ray Systems, Inc., Madison, WI, USA, 1998.
20 G. M. Sheldrick, SADABS, Siemens Area Detector Absorption Correction Program, University of Göttingen, Germany, 1996 (based on the method of R. H. Blessing, *Acta. Crystallogr., Sect. A*, 1995, **51**, 33).
21 SHELXTL version 5.03, Program for Crystal Structure Solution and Refinement, Siemens Industrial Automation, Inc., Madison, WI, USA, 1994.
22 H. D. Flack, *Acta Crystallogr., Sect. A*, 1983, **39**, 876.
23 R. Clérac, F. A. Cotton, S. P. Jeffery, C. A. Murillo and X. Wang, *Inorg. Chem.*, 2001, **40**, 1265.
24 Excess AgBF$_4$ causes oxidation of Ni$_3$(dpa)$_4$Cl$_2$, see ref. 15.
25 J. F. Berry, F. A. Cotton, T. Lu and C. A. Murillo, *Inorg. Chem.*, 2003, **42**, in press.
26 A recent special issue (*J. Organomet. Chem.*, 2003, **670**) has been devoted to the facets of acetylide chemistry.

27 For example, see: (*a*) J. A. Ramsden, W. Weng, A. M. Arif and J. A. Gladysz, *J. Am. Chem. Soc.*, 1992, **114**, 5890; (*b*) J. Pu, T. S. Peng, A. M. Arif and J. A. Gladysz, *Organometallics*, 1992, **11**, 3232; (*c*) J. A. Ramsden, W. Weng and J. A. Gladysz, *Organometallics*, 1992, **11**, 3635.
28 S. K. Hurst and T. Ren, *J. Organomet. Chem.*, 2003, **670**, 188.
29 R. Clérac, F. A. Cotton, L. M. Daniels, K. R. Dunbar, C. A. Murillo and I. Pascual, *Inorg. Chem.*, 2000, **39**, 748.
30 R. Clérac, F. A. Cotton, L. M. Daniels, K. R. Dunbar, K. Kirschbaum, C. A. Murillo, A. A. Pinkerton, A. J. Schultz and X. Wang, *J. Am. Chem. Soc.*, 2000, **122**, 6226.
31 D. M. L. Goodgame, N. J. Hill, D. F. Marsham, A. C. Skapski, M. L. Smart and P. G. H. Troughton, *Chem. Commun.*, 1969, 629.
32 R. W. Jotham, S. F. A. Kettle and J. A. Marks, *J. Chem. Soc., Dalton Trans.*, 1972, 428.